NIPES - Journal of Science and Technology Research
www.nipes.org

Optimized Removal of Zinc and Copper from Industrial Oil Mill Wastewater Using Coconut Shell-Based Activated Carbon

Nanret Liba Yaceh[1], Michael Sunday Olakunle[1], Nehemiah Samuel Maina[1], Temitope Alaba Paul-Emmanuel[2], Nandi Liba Yaceh[3]

[1]Department of Chemical Engineering, Ahmadu Bello University Zaria, Kaduna State, Nigeria. libananret@gmail.com, msmolakunle@gmail.com, nsmaina@yahoo.com,
[2]Department of Industrial and Production Engineering, University of Ibadan, Oyo State, Nigeria. starrytopsy@gmail.com
[3]Department of Architecture, University of Jos, Plateau State, Nigeria. yacehnandi@gmail.com

Article Info

Keywords: *Coconut shell activated carbon, heavy metals, biosorption efficiency, characterization, response surface methodology*

Received 02 March 2025
Revised 28 April 2025
Accepted 09 May 2025
Available online 18 May 2025

https://doi.org/10.37933/nipes/7.2.2025.12

eISSN-2682-5821, pISSN-2734-2352

Abstract

This research work basically involves the development and characterization of coconut shell activated carbon by means of chemical activation using phosphoric acid (H_3PO_4) for the removal of Zn and Cu in a batch biosorption process. Characterization of activated carbon using, surface chemistry (FTI-IR), surface area (BET) and surface morphology and elemental identification (SEM/EDX) were all carried out. This study was executed to determine the optimum biosorption efficiency parameters for Zn and Cu removal using Response Surface Methodology (RSM) to obtain maximum biosorption efficiency. The factors considered were adsorbent dosage (0.2-3 g), contact time (1-2 hrs) and temperature (25-55 ^oC), biosorption efficiency was the response. ANOVA analysis was carried out to analyse the most effective factor in experimental design response. The BET results shows the surface area was 939.16 m^2/g. SEM results showed development of good porous structure with corresponding elemental composition by the EDX. The optimum conditions for removal of Zn and Cu were adsorbent dosage 0.2 g, contact time 1 hr and temperature 40 ^oC, which shows the maximum biosorption efficiency of 88.5 % for Zn and 96.4 % for Cu removal. Isotherm models analyses showed that the biosorption process best fitted to Langmuir model with an R^2 value of 0.9935 and 0.9964 for Zn and Cu removal than that of Freundlich isotherms and also showed the biosorption process was physical. Results of the kinetic studies were best fitted by the pseudo-second order model with an R^2 value of 0.9965 and 0.9982 for Zn and Cu removal. thermodynamic studies revealed that the biosorption process was endothermic, and spontaneous.

1.0 Introduction

In recent times agricultural wastes especially those that are not consumed by animals have lithered the environment and has become a source of environmental pollution and a thing of concern. The need for development has driven so many countries into industrialization and the effect is felt on the environment, as some of these industries release toxic

effluents into the environment and water bodies. Some of these effluents such as toxic organic compound and heavy metals for example lead, zinc, arsenic, copper, chromium, cobalt, manganese cadmium, nickel and mercury have become harmful to both humans and animals if taken in large amount, and the need to reduce these toxic effluents to the barest minimum is on the increase [1]. These heavy metals are not biodegradable, they tend to accumulate in the living organisms and lead to many diseases and disorders which eventually affects human and aquatic life. They can cause ill health, even when present in the range of parts per billion (ppb) [2]. At high concentrations zinc can cause stomach cramps, skin irritation, vomiting, anaemia, pancreatitis, disturbed protein metabolism, respiratory disorders. Consumption of copper in large amount is known to be toxic and carcinogenic, causes headache, liver and kidney failure, respiratory problems and abdominal pain [3].

The need to convert some of these agricultural waste to useful sorbent to remove some of these toxic effluents from wastewater is on the rise because it is a cheaper alternative and the best practice compared to other methods such as chemical precipitation, ion exchange, chemical oxidation, reduction, reverse osmosis, electrolysis and ultrafiltration, thereby transforming environmental waste to useful product to solve environmental problems [4]. Bio-sorbent are materials of biological origin used to remove pollutants from a solution, they are biomaterials such as agricultural wastes, industrial wastes, bacterial and algae [5]. Coconut shell is usually used as an alternative to firewood in cooking and producing activated carbon which is used in wastewater treatment [6]. Activated carbon from agricultural wastes is one of the best biosorbents for heavy metal removal from wastewater, it is not only considered to be extremely effective but also easily accessible and cost-effective [7]. Activated carbon is extremely porous with a large surface area and typically produced from organic precursors such as coconut shells, palm kernel, groundnut shells, corn cob, wood chips, sawdust and seed pods [8]. Activated carbon biosorption is a process that is widely used for removal of waste from effluents, and it relies on the large surface area of the biosorbent, with its micro-porous structure, resulting in high biosorption capacity. The operation is generally simple to implement and gives high removal efficiency [9]. Previous studies have looked into the effect of different biosorption parameters, such as temperature, time, and adsorbent dosage on biosorption of heavy metals from industrial wastewater. However, they have reported high biosorbent dosage and long contact time to achieve a substantial rate of biosorption [10, 11].

This work is focused on preparing activated carbon as a biosorbent from coconut shell activated carbon through chemical activation, using phosphoric acid (H_3PO_4) for zinc and copper removal from an industrial oil mill wastewater via batch biosorption process. The purpose of this study is to reduce the spread of heavy metals within the wastewater source using an effective and efficient low-cost biosorbent from agricultural waste, the Central Composite Design (CCD) of the Response Surface Methodology (RSM) was used for modelling and optimization of the process data for the biosorption process.

2.0 Materials and Method

2.1 Materials

Analytical grade phosphoric acid (H_3PO_4) 98% w/w were purity, analytical reagent grade by BDH Chemicals was utilized for this experimental study without additional purifications. The raw material used for this study was agricultural waste (coconut shell was gotten from Zaria) and industrial oil mill wastewater.

2.2 Method

2.2.1 Proximte Analysis

Proximate analysis for coconut shell was carried out to determine, moisture content, volatile matter, ash content and fixed carbon.

2.2.2 Coconut shell activated carbon preparation

Coconut shell obtained was washed and sun dried until a constant weight was achieved using laboratory milling machine it was crushed and reduced in size.

The crushed coconut shell was charged in a crucible and transfered into a furnace set at 700°C for 1 hr at 10°C/min heating rate in N_2. The furnace was turned off and the samples were allowed to cool at room temperature after carbonization.

The acid activation of coconut shell carbon was impregnated with H_3PO_4 and the impregnation ratio between the coconut shell carbon with H_3PO_4 was (gSample /gH_3PO_4) 1:1 g/g and left overnight at room temperature.

The activated carbon was washed with distilled water many times until a neutral pH of 6.9–7 was attained; it was then left in the oven to dry at 80°C for 8 hours, then it was reduced to a particle size of 125 μm and eventually kept in an airtight container for usage.

The operating conditions of carbonization temperature and impregnation ratio implemented in this study was modified from [12].

2.2.3 Activated carbon percentage yield

The yield of activated carbon, resulting after activation of a given quantity of the carbonized coconut shell was calculated using equation 1

$$\%\ Yield = \frac{W_2}{W_1} \times 100 \quad (1)$$

Where W_2 is dry weight of final activated carbon (g) and W_1 is the dry weight of raw material (g).

2.2.4 Characterization

The coconut shell activated carbon was analyzed through Brunauer-Emmett-Teller (BET) to determine the porosity and surface area. Surface morphology was done using Scanning Electron Microscopy (SEM). Fourier transform infrared spectroscopy (FT-IR) was carried out to determine the surface chemistry, to identify the functional groups present in the sample, the spectral data were compared to a reference. X-ray Fluorescence Spectrometer (XRF) and Atomic Absorption Spectroscopy (AAS) were used to determine the elemental composition, (determination of initial concentration of metals in wastewater and final concentration of metals after biosorption).

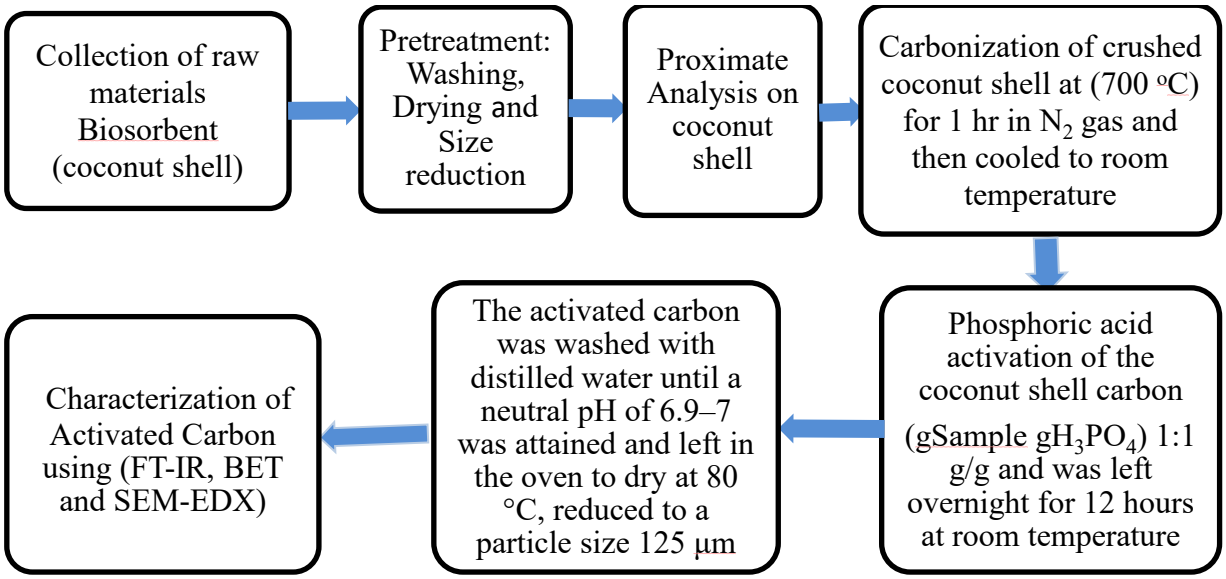

Figure 1. Block diagram showing summary of the research methodology (Dungani *et al*., (2022))

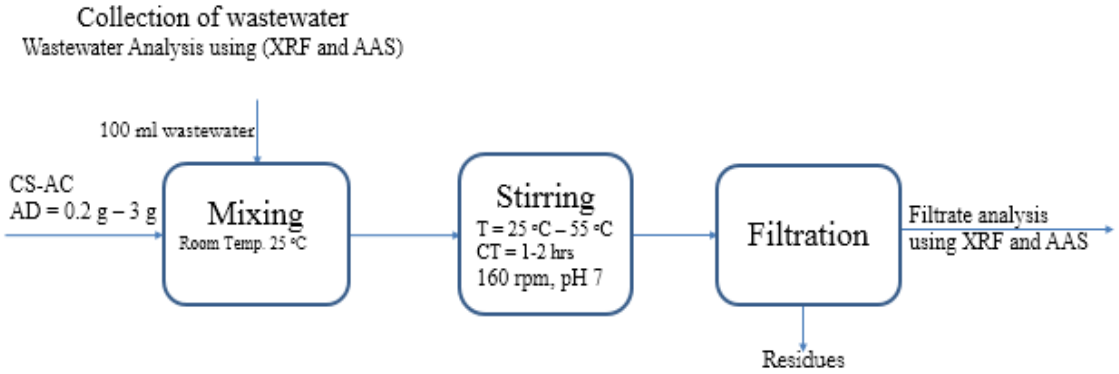

Figure 2: Batch biosorption process (Modified from Dungani *et al*., (2022))

CS-AC = Coconut Shell Activated Carbon
AD = Adsorbent Dosage
XRF = X-ray Fluorescence Analysis
T = Temperature
AAS = Atomic Absorption Spectroscopy
CT = Contact Time

2.2.5 Sorption studies

Batch biosorption studies were carried out, 100 milliliters of industrial oil mill wastewater were charged into different containers of Erlenmeyer flasks (500 mL) and 0.2 -3 g of coconut shell activated carbon were carefully measured and put into each of the containers containing the wastewater at a constant pH 6.9.

The flasks were then put into a water-bath with a stirrer set at 160 rpm speed with a varrying temperatures set within the range of 25°C -55°C for a contact time between 1-2 hrs so that equilibrium could be attained. The entire process was executed based on data generation from Central Composite Design (CCD) of Response Surface Methodology (RSM).), CCD design matrix is presented in Table 3. Before the attainment of equilibrium state, samples at different experimental time intervals were taken and then filtered by the using a micropore filter membrane (45 µm) to establish

the biosorbates remaining. The uptake of metal ions at equilibrium q, and biosorption efficiency R% were calculated as in Equations (2) and (3).

$$q = \frac{(Ci-Cf)V}{m} \quad (2)$$

where q is the metal uptake by the adsorbent (mg /g), C_i is the initial concentration of metal ion in the solution (mg /L), C_f is the final concentration of metal ion in the solution (mg /L), V is the volume of the medium (working solutions) (L), and m is the amount of the biomass (biosorbent) used in the adsorption process (g). Biosorption efficiency for the metal is given in Equation (3).

$$R\% = \frac{Ci-Cf}{Ci} \times 100 \quad (3)$$

Where R% is biosorption efficiency, C_i is the initial concentration of metal ion in the solution (mg /L), C_f is the final concentration of metal ion in the solution (mg /L) [13].

2.2.6 Experimental modelling and process optimization

The Response Surface Methodology (RSM) modelling technique was used to model the process and their performance and predictive capacity of the response (biosorption efficiency) on removal of heavy metals from industrial oil mill wastewater was examined. The experimental modeling was performed using the design expert (v12.0) software in order to determine the optimum combination and study the effect of process parameters on removal of heavy metals.

3.0 Discussion of Results

3.1 Proximate analysis

Table 1 Proximate analysis for coconut shell.

Description	% Moisture	% Ash	% Volatile Matter	% Fixed Carbon
Coconut shell	4.61	0.64	79.44	15.31

As seen from Table 1 coconut shell can serve as a very good precursor for the production of activated carbon due to its very low value in ash content (0.64%) and very high value of carbon containing constituents. According to Fletcher *et al.* [16] that materials with low moisture and ash content are a sign of good carbon material that is desirable for biosorption analysis.

3.2 Activated Carbon Percentage Yield

3.2.1 Coconut shell activated carbon percentage yield

The percentage yield of coconut shell activated carbon was obtained to be 40.11 % which reveals a significant carbon cotent in the coconut shell, this shows how much of the raw material was converted into the final product.

3.2.2. Characterization

3.3.1 Fourier-transform infrared spectroscopy (FT-IR) analysis

The FT-IR spectra in Figure 1 observed peaks at 3741 cm^{-1}, 3712 cm^{-1} and 3570 cm^{-1} was assigned to the sharp (OH) hydroxyl groups while the bands observed at around 2,959 cm^{-1} and 2,735 cm^{-1} were ascribed to broad OH and R-COOH carboxyl acids. The bands at 1,774 cm^{-1} and 1,699 cm^{-1} indicated strong C=O carbonyl acids, the peaks associated with the phosphate group (PO_4^{3-}) at 1540 cm^{-1} shows the presence of phosphorus and oxygen compounds in the sample, removal of heavy metals in these region is usually observed in carbon activated with H_3PO_4 acid. The bands at 920cm^{-1} was attributed to the strong C-H bending vibrations. FTIR result shows that the sample of coconut shell activated carbons have essential functional groups which helps in heavy metals removal.

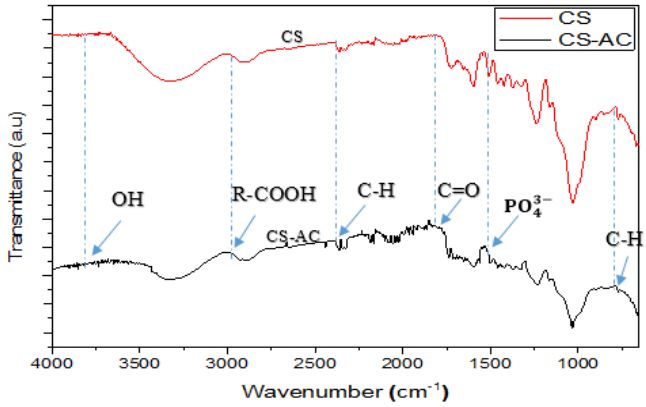

CS Coconut shell CS-AC Coconut shell activated carbon

Figure 3: FT-IR spectra of coconut shell and coconut shell activated carbon

3.3.2 Scanning electron microscopy (SEM) analysis

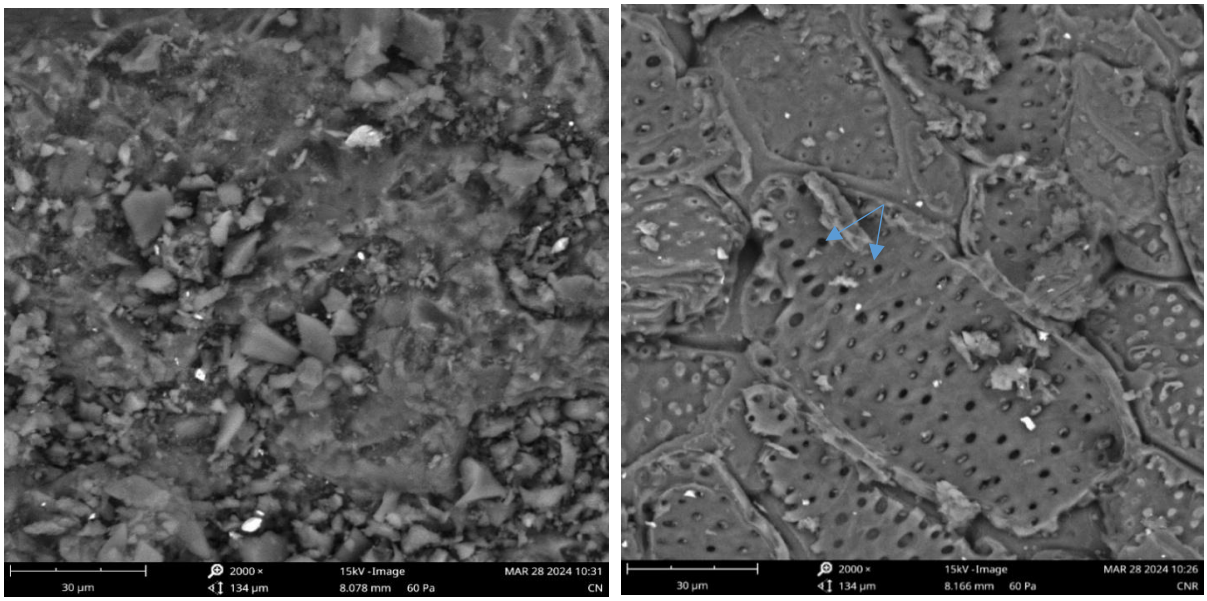

(a) (b)

Figure 4: (a) SEM images for coconut shell CS and 2(b) coconut shell activated carbon CS-AC.

CS-AC shows the development of a clear pore structure. There are many thin layers within the structure, between which are rudimentary pores owing to the release of volatiles. A system of advanced pore network was formed in the case of the CS-AC as compared to the CS leading to the rise in surface area.

These results indicated that the physical characteristics of CS-AC that was modified by carbonization and activation with H_3PO_4 to improve it and also increased the accessibility of active sites and the removal of heavy metals during the biosorption process.

Table 2: EDX Showing the elemental compositions of the coconut shell activated carbon

Element Number	**Element Symbol**	**Element Name**	**Atomic Concentration**	**Weight Concentration**
6	C	Carbon	78.12	71.67
8	O	Oxygen	17.15	20.95
7	N	Nitrogen	3.19	3.42
15	P	Phosphorus	0.50	1.18
47	Ag	Silver	0.07	0.61

13	Al	Aluminium	0.18	0.37
14	Si	Silicon	0.16	0.35
11	Na	Sodium	0.17	0.29
12	Mg	Magnesium	0.16	0.29
17	Cl	Chlorine	0.07	0.18
20	Ca	Calcium	0.06	0.17
16	S	Sulfur	0.07	0.17
26	Fe	Iron	0.03	0.12
22	Ti	Titanium	0.03	0.12
19	K	Potassium	0.04	0.11

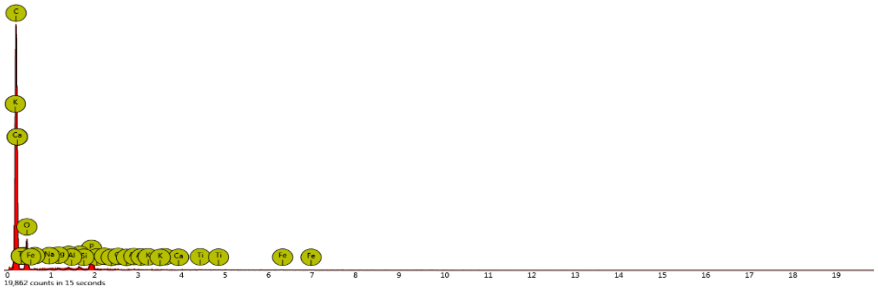

Figure 5: The EDX Image of the coconut shell activated carbon

Table 2 shows the elemental composition of coconut shell activated carbon (CS-AC). From Figure 5 EDX analysis of CS-AC, shows the peaks of carbon and oxygen are the two major peaks, which corresponds to carbon (78.12%) and oxygen (17.15%) in CS-AC. Prominent peaks of carbon (C) and oxygen (O) were observed with few subsided peaks of nitrogen (N), phosphorus (P), iron (Fe) and potassium (K) this affirm that the coconut shell activated carbon is evenly distributed with traces of carbon and oxygen due to carbonization, similar trend was seen in the works of [12].

3.3.3 Surface area (S_{BET}) analysis

Table 3. Surface area, pore size and pore volume of coconut shell activated carbon (CS-AC).

Materials	S_{BET} (m^2/g)	Pore Size (nm)	Pore Volume(cm^3/g)
Coconut shell activated carbon	939.16	3.442	0.3495

In this study, using H_3PO_4, the surface area of coconut shell activated carbon (CS-AC) was S_{BET} 939.16 m^2/g. CS-AC produced a high surface area, micropore, mesopore percentage and pore volume the values of coconut shell activated carbon surface area is in agreement with the findings of other research studies. Chen *et al*. [17] found an S_{BET} surface area of 939 m^2/g after activation of coconut shell with H_3PO_4 and carbonization at 700°C. Lutfi *et al*. [18] also reported using H_3PO_4 as an activator on activated carbon increased the pore diameter, pore volume and surface area. In this work the surface areas of CS-AC showed that chemical activation has improved the development of porosity and increased the surface area. This justify the fact that carbonization and activation not only form pores but also widens the size of the existing pores.

3.4. Response Surface Methodology

3.4.1 Modelling

The Response Surface Methodology (RSM) modelling was done according to Table 4, 5 and 7. Using the Central Composite Design (CCD) of design expert software with the ranges of parameters for each process factors considered as shown in Table 4. The generated data from design of experiment (DOE) were analyzed and optimized using the design expert software and then interpreted. The actual response values were close to the predicted values for Response Surface Methodology (RSM) for a specific experimental run. Second-order polynomial (quadratic model) was also developed based on the relationship between independent variable and the responses as shown in Table 4. Adequacy of the model was checked by analysis of variance (ANOVA), f-test, significance level of the modelled factors and coefficient of determination (R^2). Plots of response surface with contour were developed to examine the relationship between independent and dependent variables. Numerical optimization technique was also done to optimize the independent variable.

Table 4: Experimental design matrix for biosorption efficiency of Zn and Cu removal with the RSM modelling techniques

Runs	Factor 1 A: Adsorbent dosage (grams)	Factor 2 B: Temperature (°C)	Factor 3 C: Time (hour)	Biosorption Efficiency %			
				Experimental		RSM Pridicted	
				Zn	Cu	Zn	Cu
1	1.6	40	1.5	82.5	85.2	82.4	85.4
2	1.6	40	1.5	83.4	85.1	83.1	85.3
3	1.6	65.2269	1.5	67.4	76	66.5	76.3
4	1.6	40	1.5	82.5	85.2	83	85.3
5	3.95451	40	1.5	81.2	67.8	80.4	68.5
6	0.2	55	2	67.3	94.8	68.4	94.5
7	0.2	25	2	68.3	80.3	69.6	79.6
8	3	55	1	70.5	70.9	70.1	70.8
9	1.6	14.7731	1.5	64.1	69.2	64.3	70.4
10	1.6	40	1.5	82.9	85.3	82.7	85.5
11	1.6	40	0.659104	83.3	81	83.6	82.2
12	1.6	40	1.5	83.5	85.4	83.4	85.6
13	3	25	2	83.7	83.7	84.3	83.5
14	1.6	40	2.3409	83.9	87.9	82.3	86.3
15	1.6	40	1.5	84.1	85.2	83.8	85.1
16	0.2	25	1	77.5	75.9	76.4	75.4
17	3	55	2	69.1	68.9	69.9	69.3
18	3	25	1	74.4	80.7	73.1	80.3
19	0.02	40	1.5	61.2	62.1	60.1	63.3
20	0.2	55	1	87.1	95.1	87.7	95.3

3.4.2. Analysis of Variance (ANOVA) on biosorption efficiency for Zn and Cu removal

Table 5 and 7 shows the ANOVA table for the level of significance of each of the modelled factors on biosorption efficiency for Zn and Cu removal. For Zn removal, Table 5 shows the individual parameter (A-adsorbent dosage, B-temperature and C-time) has a significant level of influence in determining the biosorption efficiency as seen from the F-value of 9, 12 and 6.38 respectively likewise the interactive effect of these process parameters (AB, AC, BC, A^2, B^2) shows significant level in the biosorption process as compared to C^2 which is not significant with F-value of 1.32.

For Cu removal, Table 7 shows that the individual parameter (A-adsorbent dosage, B-temperature and C-time) has a significant level of influence in determining the biosorption efficiency with the F-value of 43.22, 10.78 and 8.16 respectively likewise the interactive effect of these process parameters (AB, AC, BC, A^2, B^2) shows significant level in the biosorption process as compared to C^2 which is not significant with F-value of 1.4054.

Table 6 showing the fit statistics with value of R^2= 0.9871 for Zn removal and Table 8 showing the fit statistics with value of R^2= 0.9902 for Cu removal which is near unity signifying limited errors from the model. The plot of predicted vs actual values from Figure 6 and Figure 7 also confirmed that no much error was observed from the modelling. For a good fit of a model Aklilu [19] recommend that R^2 value should be at least 0.80 [19]. The value of the adjusted R^2 for biosorption efficiency was 0.9755 and 0.9814 for Zn and Cu removal, which certify that the model was very important, suggesting good agreement between the experimental and predicted values of the response variables. Owolabi *et al.* [20] suggested that adjusted R^2 and predicted R^2 should be within 20% to be in good concession [20].

Modelled equation of biosorption efficiency for Zinc (Zn) removal

Biosorption efficiency = 1.18232 + 0.529664*A + 3.52748*B + 18.07034*C – 0.182758*A*B + 5.86542*A*C – 0.512643*B*C – 0.624033* A^2 – 0.030899* B^2 – 3.12403* C^2 (4)

Where A= Adsorbent dosage, B= Temperature and C= Time

Modelled equation of biosorption efficiency for Copper (Cu) removal

Biosorption efficiency = 1.14128 + 14.78738*A + 2.76109*B + 22.29353*C – 0.368322*A*B –1.23446*A*C – 0.315504*B*C – 0.762806* A^2 – 0.019787* B^2 – 1.58840* C^2 (5)

Where A= Adsorbent dosage, B= Temperature and C= Time

Table 5: ANOVA for quadratic model for Zn removal

Source	**Sum of Squares**	**Df**	**Mean Square**	**F-Value**	**P-Value**	
Model	923.33	9	135.93	84.88	< 0.0001	Significant
A-Adsorbent dosage	74	1	74	9	< 0.0001	
B-Temperature	75	1	75	12	0.0005	
C-Time	20.67	1	20.67	6.38	0.0011	
AB	124.50	1	124.50	14.36	0.00035	
AC	144.65	1	144.65	16.68	0.0022	
BC	187.31	1	187.31	21.6	0.0009	
A^2	12.59	1	12.59	3.45	0.0015	
B^2	808.05	1	808.05	93.20	< 0.0001	
C^2	11.43	1	11.43	1.32	0.0032	
Residual	8.69	10	8.67			
Lack of Fit	6.88	5	1.38	1.71	0.0037	not significant
Pure Error	1.81	5	0.9627			
Cor Total	932.02	19				

Table 6: Fit statistics from the ANOVA for Zn removal

Std. Dev.	2.94	**R^2**	0.9871
Mean	73.72	**Adjusted R^2**	0.9755
C.V. %	3.99	**Predicted R^2**	0.9253
		Adeq Precision	41.5630

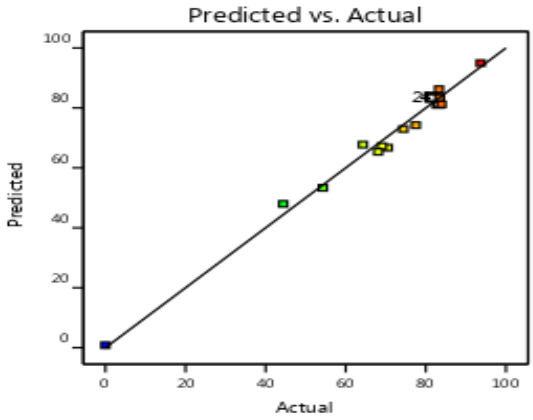

Figure 6 The predicted values versus the actual values of biosorption efficiency for Zn removal.

Table 7: ANOVA for quadratic model for Cu removal

Source	**Sum of Squares**	**Df**	**Mean Square**	**F-Value**	**P-Value**	
Model	889.27	9	232.81	112.29	< 0.0001	Significant
A-Adsorbent dosage	314.79	1	314.79	43.22	< 0.0001	
B-Temperature	42.07	1	42.07	10.78	0.0037	
C-Time	30.29	1	30.29	8.16	0.0068	
AB	505.66	1	505.66	69.43	<0.0001	
AC	36.41	1	36.41	8.798	0.0037	
BC	70.95	1	70.95	9.74	0.0050	
A^2	24.81	1	24.81	7.58	0.0139	
B^2	331.34	1	331.34	45.49	< 0.0001	
C^2	12.31	1	12.31	1.4057	0.0538	
Residual	9.87	10	7.28			
Lack of Fit	8.86	5	6.37	4.057	0.0243	not significant

Pure Error	1.01	5	0.1017			
Cor Total	899.14	19				

Table 8: Fit statistics from the ANOVA for Cu removal

Std. Dev.	2.70	**R^2**	0.9902
Mean	77.17	**Adjusted R^2**	0.9814
C.V. %	3.50	**Predicted R^2**	0.8593
		Adeq Precision	49.2516

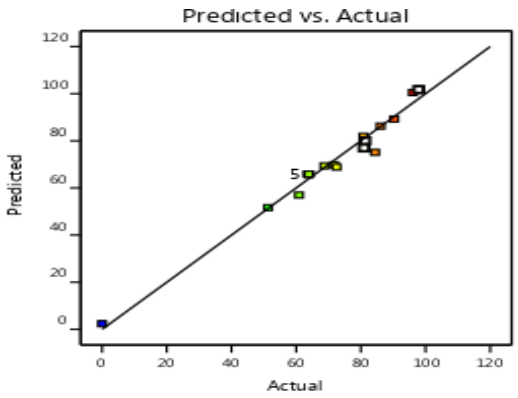

Figure 7 The predicted values versus the actual values of biosorption efficiency for Cu removal.

3.4.3 Optimization

Process optimization was done for the process factors (Adsorbent dosage, Temperature and Time) and the RSM Optimal process conditions for maximum biosorption efficiency for biosorption of heavy metals are summarized in Table 9 and Table 10 respectively. Chen *et al*. [17], reported that removing 80 % of heavy metals from industrial wastewater offers significant benefits for both human health and the environment. This reduction minimizes the risks linked with heavy metal exposure, protects human and aquatic life, and helps prevent soil contamination [17].

3.4.4. RSM optimal conditions and biosorption efficiency for Zn and Cu removal

Table 9: Process factors for optimization and optimal responses for Zn and Cu removal

Factors	**Zn**	**Optimal Responses**	**Cu**	**Optimal Responses**
Adsorbent dosage (grams)	Range	0.200	Range	0.200
Temperature (^{o}C)	Range	40.01	Range	40.00
Time(hrs)	Range	1.000	Range	1.001
Biosorption Efficiency (%)	Maximum	88.497	Maximum	96.4325
Desirability	1.0		1.0	

Table 10: Response Surface Methodology (RSM) optimal conditions and biosorption efficiency.

Adsorbent dosage (g)	Temperature (^{o}C)	Time (hr)	Biosorption Efficiency			
			RSM Predicted		Experimental	
			Zn	Cu	Zn	Cu
0.200	40.01	1.001	87.7	95.3	88.497	96.433

The plots from Figure 8a and 8b shows the three-dimensional surface plots after optimization for the combined effects of adsorbent dosage, temperature and time on biosorption efficiency at the optimal RSM values for Zn and Cu removal, this signifies that biosorption efficiency increases with temperature increase above 40 °C and decreases with increasing adsorbent dosage.

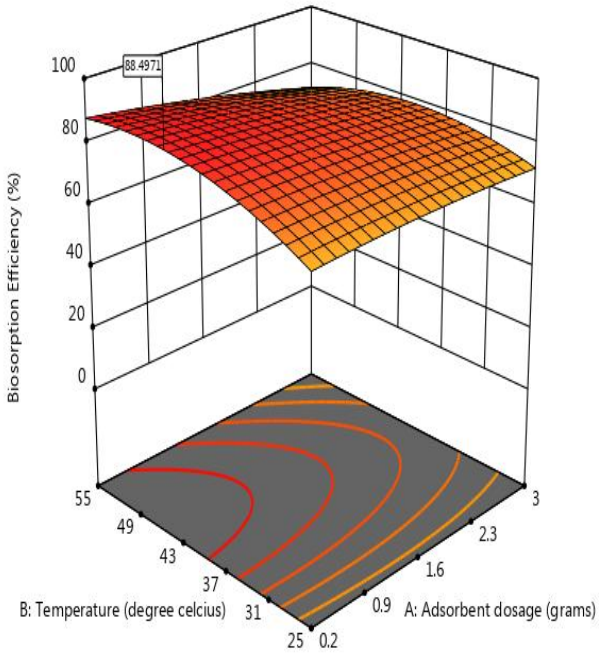

Figure 8a

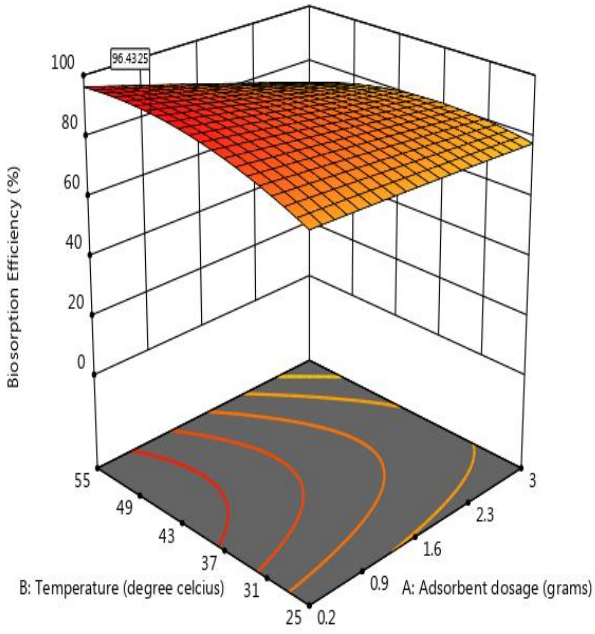

Figure 8b

Figure 8a and 8b: Three-dimensional surface plot for effect of temperature and adsorbent dosage on biosorption efficiency at constant time 1hr for Zn and Cu removal.

3.5. Adsorption Isotherm Studies

3.5.1. Langmuir and Freundlich adsorption isotherm for Zn and Cu removal

Figure 9 shows the plot of Ce/qe vs Ce fitted well for Zn removal and gave a linear plot with correlation coefficient of R^2=0.9935 and a root mean square error (RMSE=0.162). The slope and intercept of the plot was used to calculate other Langmuir isotherm parameters which include q_m (mg/g), K_L (L/mg) and R_L. Adsorption value q_m and K_L values shows maximum biosorption of Zn on the surface of the biosorbent with the Langmuir isotherm model as compared with the Freundlich isotherm model.

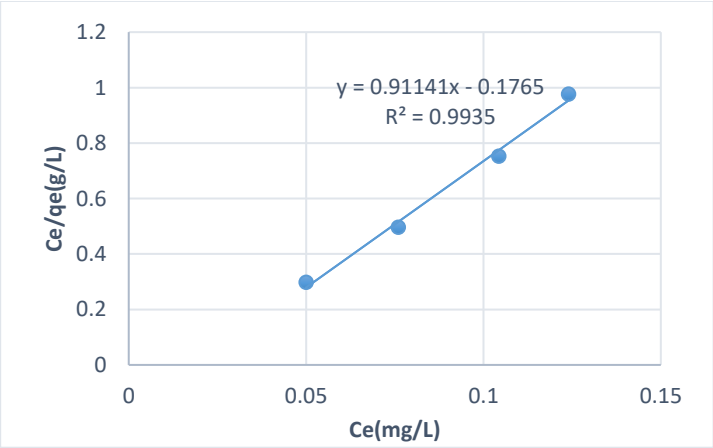

Figure 9: Langmuir adsorption isotherm plot showing Ce/qe vs Ce for Zn removal

Figure 10 shows plot of ln qe vs ln Ce for Zn removal gave line with R^2 = 0.9631 and RMSE=0.483. Freundlich parameters K_F and n was also calculated from the slope and intercept of the curve.

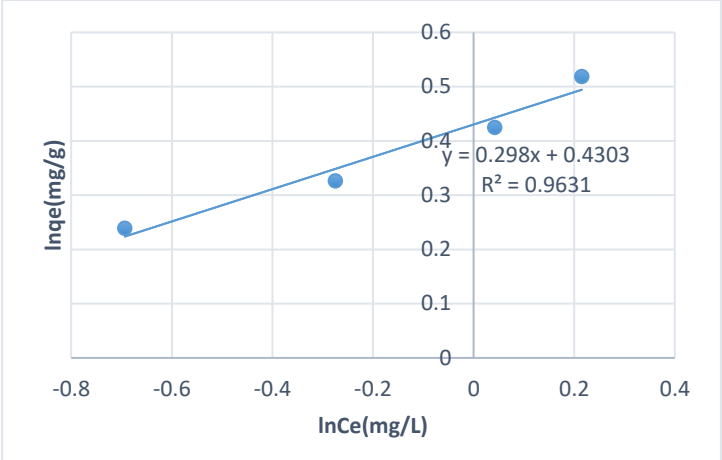

Figure 10: Freundlich adsorption isotherm plot showing ln qe vs ln Ce for Zn removal

The plot of Ce/qe vs Ce fitted well for Cu removal and gave a linear plot with R^2=0.9964 as represented in (Figure 11) and RMSE=0.218. The slope and intercept of the plot was used to calculate other Langmuir isotherm parameters which include $q_{m\ (}$mg/g), $K_{L\ (}$L/mg) and R_L. Adsorption value q_m and K_L values shows maximum biosorption of Cu on the surface of the biosorbent with the Langmuir isotherm model as compared with the Freundlich isotherm model.

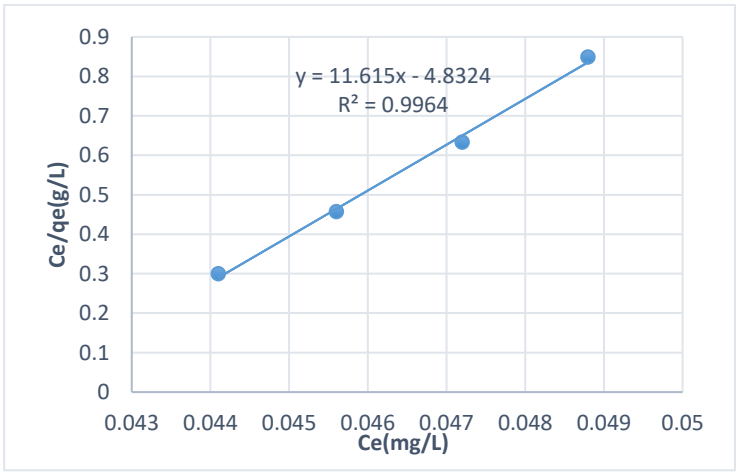

Figure 11: Langmuir adsorption isotherm plot showing Ce/qe vs Ce for Cu removal

Figure 12 shows a plot of ln qe vs ln Ce for Cu removal gave a line with R^2 = 0.9287 and RMSE=0.654. The Freundlich parameters K_F and n was also calculated from the slope and intercept of the curve.

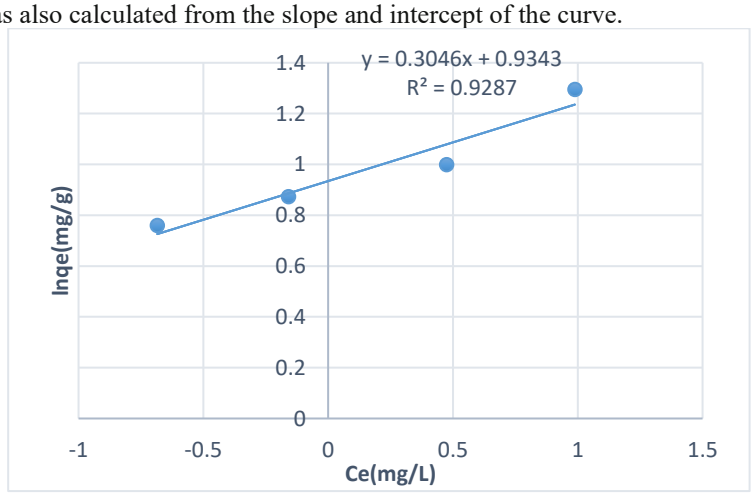

Figure 12: Freundlich adsorption isotherm plot showing ln qe vs ln Ce for Cu removal

Plot results from the above two models shows that Langmuir isotherm with higher R^2 close to unity and lowest RMSE value of 0.162 for Zn and 0.218 for Cu fits quite well with the experimental data and the model can best describe the adsorption process, whereas the low R^2 and higher RMSE show poor agreement of the Freundlich isotherm with the experimental data.

Table 11: Biosorption isotherms for Zn and Cu removal using coconut shell activated carbon

Isotherms	Metals	Model	Linear Form	Plots	Kinetic Parameters
Langmuir	Zn	$q_e = \frac{q_m K L C_e}{1 + K L C_e}$	$\frac{C_e}{q_e} = \frac{1}{q_m K L} + \frac{C_e}{q_m}$	Ce/qe vs Ce	q_m=1.0972 mg/g K_L=0.5202 L/mg R_L=0.7936 R^2=0.9935
Freundlich	Zn	$q_e = K_F C_e^{\frac{1}{n}}$	$\ln q_e = \ln K_F + \frac{1}{n} \ln C_e$	ln qe vs ln Ce	K_F=1.3472 mg/g n=2.324 R^2= 0.9631
Langmuir	Cu	$q_e = \frac{q_m K L C_e}{1 + K L C_e}$	$\frac{C_e}{q_e} = \frac{1}{q_m K L} + \frac{C_e}{q_m}$	Ce/qe vs Ce	q_m=0.8609 mg/g K_L=0.4504 L/mg R_L=0.8905 R^2=0.9964
Freundlich	Cu	$q_e = K_F C_e^{\frac{1}{n}}$	$\ln q_e = \ln K_F + \frac{1}{n} \ln C_e$	ln qe vs ln Ce	K_F=1.3561 mg/g n=1.070 R^2= 0.9287

3.6 Kinetic Study

For lagergren pseudo-first order, linear curve of the plot was analysed and correlation coefficient of R^2 = 0.9234 and 0.9716 for Zn and Cu removal respectively were obtained alongside the following parameters, k_1 min^{-1} and q_e mg/g. For the pseudo-second-order kinetic model a linear plot of qt vs t was evaluated as shown in Figure 14 which gave R^2=0.9965 and 0.9982 for Zn and Cu removal and the following second order parameters were obtained; K_2 ($gmg^{-1}min^{-1}$), q_e (mg/g) and qe_{exp} The analyzed values of the R^2 for Pseudo-second order model was near to unity with the value higher making it fit well than the first order model. The calculated qe values matched well with the experimental value for the pseudo second order model, demonstrating that biosorption of Zn and Cu followed a pseudo second order rate expression.

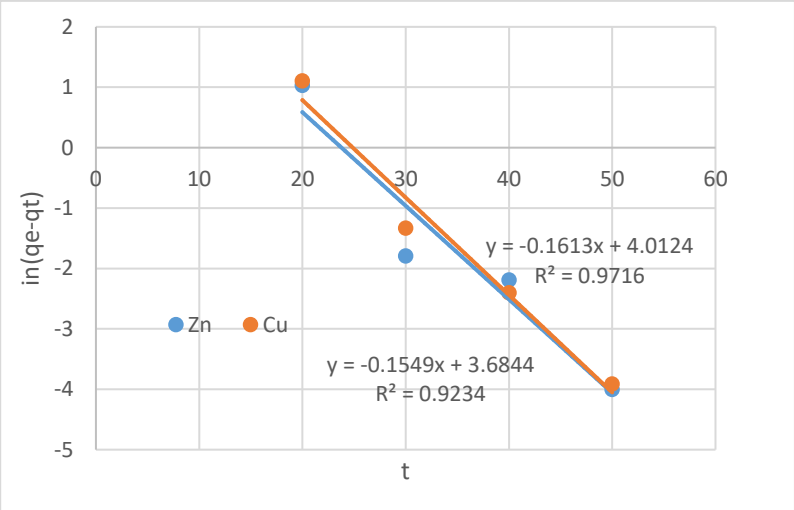

Figure 13: Plot of lagergren pseudo-first order Zn and Cu removal

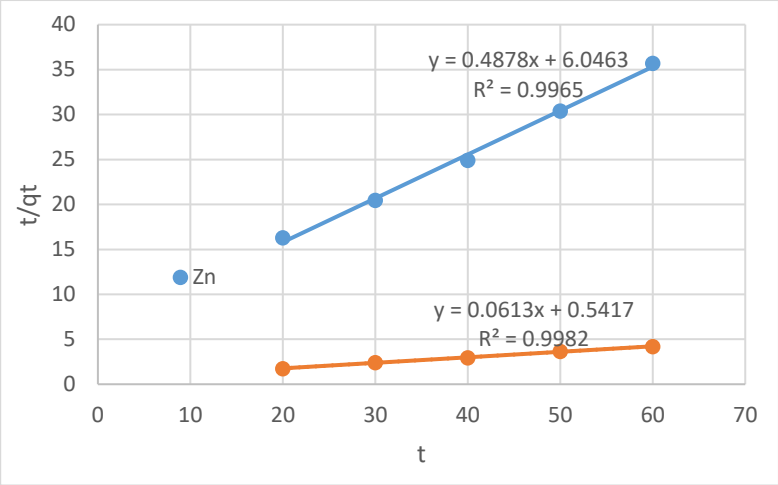

Figure 14: Plot of lagergren pseudo-second order for Zn and Cu removal

Table 12 shows summary of values of the parameters obtained from these two kinetic models. In conclusion, the K_2 values of pseudo second order kinetics is also found lower than that of the K_1 values of the first order as well as the closeness of the qe_{cal} and qe_{exp} suggest the adequacy of the pseudo second order reaction model for the biosorption reaction compared to the pseudo first order for the removal of Zn and Cu.

Table 12: Kinetic Study Zn and Cu removal using coconut shell activated carbon

Model	**Metals**	**Model Equation**	**Plots**	**Kinetic parameters**
Lagergren First-order	Zn	$\ln(qe-qt) = \ln qe - k_1 t$	ln(qe-qt) vs t	k_1 (min^{-1}) = 0.1549 q_e (mg/g) =40.06 R^2 = 0.9234
Pseudo second-order	Zn	$\frac{t}{qt} = \frac{1}{k_2 qe^2} + \frac{t}{qe}$	t/qt Vs t	k_2 ($gmg^{-1}min^{-1}$) = 0.03934 qe_{cal} (mg/g) = 12.050 qe_{exp} = 12.034 R^2= 0.9965
Lagergren First-order	Cu	$\ln(qe-qt) = \ln qe - k_1 t$	ln(qe-qt) vs t	k_1 (min^{-1}) = 0.1613 q_e (mg/g) =55.28 R^2 = 0.9716
Pseudo second-order	Cu	$\frac{t}{qt} = \frac{1}{k_2 qe^2} + \frac{t}{qe}$	t/qt Vs t	k_2 ($gmg^{-1}min^{-1}$) = 0.00694 qe_{cal} (mg/g) = 16.31 qe_{exp} = 16.28 R^2=0.9982

3.7 Thermodynamic Parameters

The enthalpy (ΔH^o) and entropy (ΔS^o) changes of the process was determined from the slope and intercept of the line obtained by plotting $\ln k_d$ versus 1/T in Figure 15.

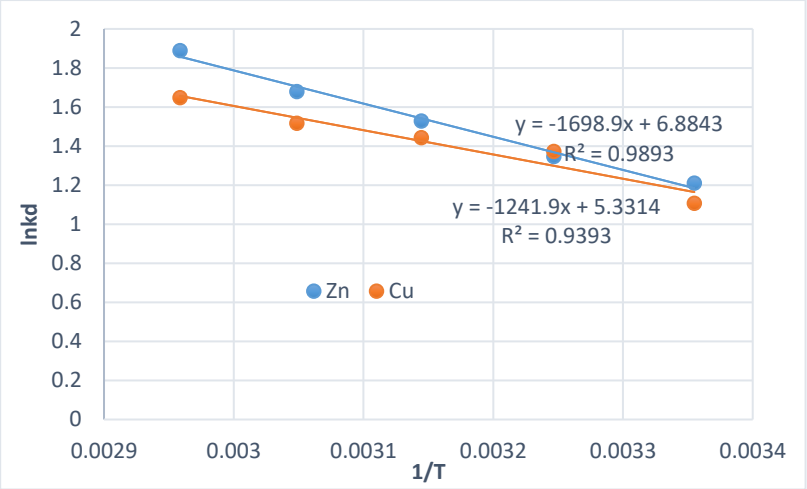

Figure 15: Plot of ln k_d Vs 1/T for Zn and Cu removal

Thermodynamic parameters (ΔG°, ΔS°, ΔH°) is shown in Table 13 at different temperatures 298K, 308K, 318K, 328K and 338K. The negative ΔG° values which is reducing as the temperature is increasing shows that the reaction was thermodynamically feasible and spontaneous while the positive enthalpy (ΔH°) and entropy (ΔS°) values confirmed the endothermic character of the biosorption process and the increasing order or randomness at the solid-liquid interface during the biosorption process respectively.

Table 13: Thermodynamic analysis parameters for Zn and Cu removal

Metals	T(K)	ΔG° (kJ/mol)	ΔS° (kJ/molK)	ΔH° (kJ/mol)
Zn	298	-2.93291	0.05724	14.1246
	308	-3.50532		
	318	-4.07775		
	328	-4.65012		
	338	-5.22253		
Cu	298	-2.88216	0.044325	10.3252
	308	-3.28043		
	318	-3.76857		
	328	-4.21176		
	338	-4.65492		

4.0. Conclusion

This study shows that a good biosorbent was produced from coconut shell through phosphoric acid activation with a good surface area, the FT-IR result shows peaks of important functional groups such as the OH, C-H, PO_4^{2-} C=O, R-COOH carbonyl and carboxyl groups which are needed for heavy metals removal during biosorption process. Activation of coconut shell carbon gave a high surface area S_{BET} 939.16 m^2/g with an average pore size of 3.442 nm and pore volume of 0.3495 cm^3/g. SEM results showed development of good porous structure as a result of activation with H_3PO_4. The optimum condition for removal of Zn and Cu was adsorbent dosage 0.2 g, contact time 1 hr and temperature 40 °C, which shows the maximum biosorption efficiency of 88.5 % for Zn and 96.4 % for Cu removal, the high biosorption efficiency of the coconut shell activated carbon makes it a better choice to be utilize than other commercial adsorbents for heavy metals removal. Industrial scale-up can be done by optimizing activated carbon production and wastewater treatment processes executing cost analysis and environmental impact for a more efficient process.
The Langmuir isotherm with an R^2 value of 0.9935 and 0.9964 for Zn and Cu removal fits well with the experimental data and is higher than that of Freundlich isotherms which may be due to homogenous distribution on the active sites of the biosorbents. Kinetics data were best fitted by the pseudo-second order model with an R^2 value of 0.9965 and 0.9982 for Zn and Cu removal, thermodynamics parameters show positive enthalpy and entropy for Zn and Cu removal and negative ΔG° values which is reducing as the temperature is increasing indicated that the biosorption process was endothermic and spontaneous in nature.

References

[1] Tripathi A. and Ranjan M. R. (2015). Heavy Metal Removal from Wastewater Using Low Cost Adsorbents. *J Bioremed Biodeg.*, 6, 3-15. doi:10.4172/2155-6199.1000315

[2] Fu, Z., Guo, W., Dang, Z., Hu, Q., Wu, F., Feng, C., Zhao, X., Meng, W., Xing, B. and Giesy, J.P. (2017). Refocusing on nonpriority toxic metals in the aquatic environment in China. *Environmental Science & Technology*, 51, 3117–3118.

[3] Agarwal, M. and Singh, K. (2017). Heavy metal removal from wastewater using various adsorbents: a review. *Journal of Water Reuse and Desalination*,7(4), 387–419.

[4] Kanamarlapudi S. L. R. K., Chintalpudi V. K. and Muddada S., (2018). Application of Biosorption for Removal of Heavy Metals from Wastewater. *IntechOpen*, DOI: 10.5772/intechopen.77315.

[5] Adewuyi A. (2020). Chemically Modified Biosorbents and Their Role in Removal of Emerging Pharmaceutical Waste in the Water System. A Review. *Water*, 12(6) 15-51

[6] Jekayinfa S. O., Orisaleye J. I. and Pecenka R. (2020). An Assessment of Potential Resources for Biomass Energy in Nigeria. *Resources*, 9 (92): 11-15. doi:10.3390/resources9080092

[7] Singh K. and Waziri, S. A., (2019). Activated carbons precursor to corncob and coconut shell in the remediation of heavy metals from oil refinery wastewater. *Journal of Materials and Environmental Sciences*, 10(7) 657-667

[8] Dika J. (2015). Production of activated carbon from combined precursor raw materials (coconut shell and sawdust). 8:9-12

[9] Olawale A. S., Ajayi O. A., Olakunle M. S., Ityokumbul M.T. and Adefila S. S. (2015). "Preparation of phosphoric acid activated carbons from Canarium Schweinfurthii Nutshell and its role in methylene blue adsorption" *Journal of Chemical Engineering and Material Science*: Vol. 6(2) 9-14. DOI: 10.5897/JCEMS2015.0219

[10] Aminul Islam and Imran Kabir (2016). Application of Coconut Shells Activated Carbon for Heavy Metal Removal from Wastewater. *American-Eurasian Journal of Toxicological Sciences*, 8(2):77-82. DOI:10.5829/idosi.aejts.2016.8.2.102198

[11] Packialakshmi S., Anuradha B., Nagamani K., Sarala Devi J. and Sujatha S. (2021). Treatment of industrial wastewater using coconut shell based activated carbon. *Materials Today: Proceedings,* 30(40) 30 https://doi.org/10.1016/j.matpr.2021.4.548

[12] Dungani R., Munawar S. S., Karliati T., Malik J., Pingkan Aditiawati P. and Sulistyono S. (2022). Study of Characterization of Activated Carbon from Coconut Shells on Various Particle Scales as Filler Agent in Composite Materials. *Journal of the Korean Wood Science and Technology*, 50(4): 256-271. https://doi.org/10.5658/WOOD.2022.50.4.256

[13] Todorova K., Velkova Z., Stoytcheva M., Kirova G., Kostadinova S. and Gochev V., (2019). Novel composite biosorbent from Bacillus cereus for heavy metals removal from aqueous solutions. *Biotechnology and Botechnological Equipment*, 33(1), 730-738. DOI: 10.1080/13102818.2019.1610066

[14] Uddin M. K., and Nasar A. (2020). Walnut shell powder as a low-cost adsorbent for methylene blue dye: isotherm, kinetics, thermodynamics, desorption and response surface methodology examinations. *Sci Rep* 10, 7983. DOI:10.1038/s41598-020-64745-3

[15] Elhadj M., Samira A., Mohamed T., Djawad F. and Asma A. (2019). Removal of Basic Red 46 dye from aqueous solution by adsorption and photocatalysis: equilibrium, isotherms, kinetics and thermodynamic studies. *Separation Science and Technology*, 1-17, https://doi.org/10.1080/01496395.2019.1577896.

[16] Fletcher A., Somorin T., Aladeokin O. (2023) Production of High Surface Area Activated Carbon from Peanut Shell by Chemical Activation with Zinc Chloride: Optimization and Characterization. *Bionerg. Res.* 17, 467-478, https://doi.org/10.1007/s12155-023-10683-7

[17] Chen Y., Zhou L., Hong Y. Z., Cao F., Li L. and Li J. B. (2022). Preparation of high-surface-area activated carbon from coconut shells. *J. Carbon*, 48(10):3005-3006 DOI: 10.1016/j.carbon.2022.03.059

[18] Lutfi M., Bambang S. Prasetyo J. and Hanafi N. (2021). Characteristics of coconut shell (Cocos nucifera) through chemical activation process. *Earth and Environmental Science*, 733: 012134. DOI:10.1088/1755-1315/733/1/012134

[19] Aklilu E. G. (2021). Artificial Neural Networks (ANNs) and Response Surface Methodology (RSM) Approach for Modeling and Optimization of pectin extraction from banana peel. 1-34, DOI:10.21203/rs.3.rs-102634/v1

[20] Owolabi, R. U., Usman, M. A. and Kehinde, A. J. (2016). Modelling and optimization of process variables for the solution polymerization of styrene using response surface methodology. *Journal of King Saud University - Engineering Sciences*, 30(1), 22–30. https://doi.org/10.1016/j.jksues.2015.12.005